

A Hybrid Embedded System Design for Real Time Monitoring the Detection of Diseases and Nutrients Deficiency in Oryza Sativa L Using LabVIEW

R. Maheswaran

Research Scholar,
Research and development center, Dept. of Electronics and Instrumentation
Bharathiar University,
Coimbatore District
mahesdei@gmail.com

S. Muruganand

Assistant Professor
Bharathiar University,
Coimbatore District
drsmbu2010@gmail.com

C. Hemalatha

Research Scholar,
Dept. of Electronics and Instrumentation
Bharathiar University,
Coimbatore District
hemal2019@gmail.com

Abstract- In recent days, world population is incredibly growing. Day by day the need of food is increasing. Drought and water scarcity are the major problems that every farmer faces today. Farmers cannot detect the nutrients deficiency and diseases in paddy field at the earliest. Farmers prefer other businesses rather than agriculture so the productivity is going down. Plant cultivation is always under surveillance using wireless IP camera. In this paper, texture features are extracted using GLCM and Mean, Standard deviation, Kurtosis and Skewness. K- Nearest Neighbor (KNN) and Support Vector Machine (GRBF) are used for classifications. This paper is used to identify the deficiency part in the crop leaf. Nowadays leaf analysis is one of the innovative researches for many applications. Every plant and crop production need nutrient for their growth. Totally 16 nutrients are required for crop growth. The proposed system implements a novel approach to identify the lack of nutrients in the crop image. Images are collected from the open source. The input images are processed in three steps: preprocessing, feature extraction and regression. In the preprocessing, HSV transformation and histogram enhancement are processed. The objective of proposed research is to monitor the disease and plant nutrition deficiency in crops. This idea saves lot of man power, increases the quality with quantity and feasible for precision agriculture.

Keywords: LabVIEW, Image Processing, KNN, SVM, HSV, precision Agriculture.

Introduction

A Paddy is the most important crops in the world. India is the second largest producer of paddy in world [1]. In Paddy field, the diseases can be prevented and managed if the symptoms are identified in the early stages also finds Nutrients deficiency. So this research work aims to focus on hybrid embedded system design for monitoring the detecting the diseases and nutrients deficiency in Oryza Sativa L in real time. We must prevent Paddy diseases for increasing the quantity and quality. The diseases which often affect the Paddy are Zinc deficiency and Mycorellosiellaoryzae. Due to the increasing costs of crop production and to the progressing environmental pollution by agrochemicals, mineral fertilizers should be applied more efficiently. This concerns primarily N, because the over application of this element leads to low N recovery efficiency and to a risk of nitrate pollution of ground

waters. The diagnostics of disease symptoms in plants, including those resulting from nutrient deficiencies, require quick, reliable and precise instrumental techniques enabling to recognize the symptoms of physiological disorders prior to the occurrence of responses to stress factors that can be observed visually. The majority of them affect the composition and proportions of pigments in leaf tissues [2].

For growth and development, plants need some food. Each plant wants 16 essential elements for its development. They are Carbon, hydrogen, and oxygen are derived from the atmosphere and soil water and the remaining 13 elements are nitrogen, phosphorus, potassium, calcium, magnesium, sulfur, iron, zinc, manganese, copper, boron, molybdenum, and chlorine. Based on soil minerals and soil organic matter these are supplied by organic and inorganic fertilizer. [3]

If the nitrogen supply is decreases in plant then the relative growth rate (RGR) for the respective plant is decreased. This type of decrease is mainly happened through decreases in leaf area ratio (LAR). It is also depending on the lower leaf mass ratio (LMR), but it is not usual and also decreases in specific leaf area (SLA) [4 and 5].

Some of the nutrients in plants are changed. In [6] the author tells about the concentration of nitrate in soils and their changes. This type of concentration is affected by two processes they are denitrification and leaching. Denitrification is happen when the soil is undertaken with water temporarily and the oxygen part is removed from the soil pores. Leaching of nitrate occurs in soils when excessive water moves through the profile, especially sandy soils.

Related Work

SantanuPhadikar et al. [7] proposed a rice diseases classification using feature selection and rule generation techniques. This paper focused on classifying from the infected regions in the rice plant image. Symptoms of the diseases are colour, shape and position of the infected portion and extracted by developing novel algorithms.

Gonzalez R.C et al. [8] Noise removal process is one of the pre-processing steps in image processing. So it is very important to remove the noise from the digital images for further process. In literature many filters were used to remove the salt and pepper noise. The most popular method to remove impulse noise is median filter (MED).

Haralick et al. [9] extracted a fourteen texture features from GLCM. From this five important features which were

contrast, entropy, energy, correlation and homogeneity were extracted. And First-order histogram based features such as mean, standard deviation, kurtosis and skewness were extracted.

J. Du, D. Huang et al [10] Plant species identification is carried over the author proposed an efficient algorithm to detect the leaf by using computer-aided plant species identification and this system is depend on the shape of the leaf images.

Lemaire et al [11] Nevertheless, standard laboratory analysis of N concentration in the above-ground biomass is expensive and time consuming; especially if a rapid crop N status evaluation is required for in-season decision making procedures. For this reason, quick and practical tests have been proposed, some of which are already spread among growers. Opto-electronic based techniques can strongly help to reach the previously mentioned goals, thanks to easiness of use and low costs. Two of the most common and simple of these are: the chlorophyll meter readings (e.g., SPAD-502, Minolta) and the measurements of N-NO₃ concentration in petiole sap (SAP test).

Netto, A.T et al [12] studied the color of robusta (Coffea canephora Pierce ex Froehner) leaves, and noted the occurrence of a significant linear dependence between the N content of leaves and readings on a chlorophyll meter

Carter et al [11] analyzed leaf spectral reflectance, transmittance and absorbance under conditions of physiological stress in five plant species, and reported that the greatest differences occurred at wavelengths around 700 nm. The most significant changes in reflectance concerned the yellow-green color, which was ascribed to the effect of stress on a decrease in the chlorophyll content of leaves. However, in some cases these changes were not specific to particular stress factors, implying the need to continue research into changes in the color of leaves in plants exposed to stressors.

Materials and Method

The median of the pixel values in the window is computed and the center pixel of the window is replaced with the computed median. Median filtering is done by, first sorting all the pixel values from the surrounding neighborhood into numerical order and then replacing the pixel being considered with the middle pixel value. Note that the median value must be written to a separate array or buffer so that the results are not corrupted as the process is performed. Figure 1 illustrates the methodology.

323	325	326	330	340
322	324	326	327	335
318	320	350	325	334
319	315	319	323	133
311	316	310	320	330

Fig.1. Concept of Median Filtering

Neighbourhood values 315,320,324,326,327,325,323,319,350 and Median value is 327. The central pixel value of 350 in the 3×3 window shown in Figure 3.3 is rather unrepresentative of the surrounding pixels and is replaced with the median value of 327. A single very unrepresentative pixel in a neighbourhood will not affect the median value significantly. Since the median value must actually be the value of one of the pixels in the neighbourhood, the median filter does not create new unrealistic pixel values when the filter straddles an edge. For this reason the median filter is much better at preserving sharp edges. In this present study median filter uses 3x3 filtering window. It has high efficiency to suppress the noise. The median filter is a non-linear filter and it works best with noise whilst retaining sharp edges in the image.

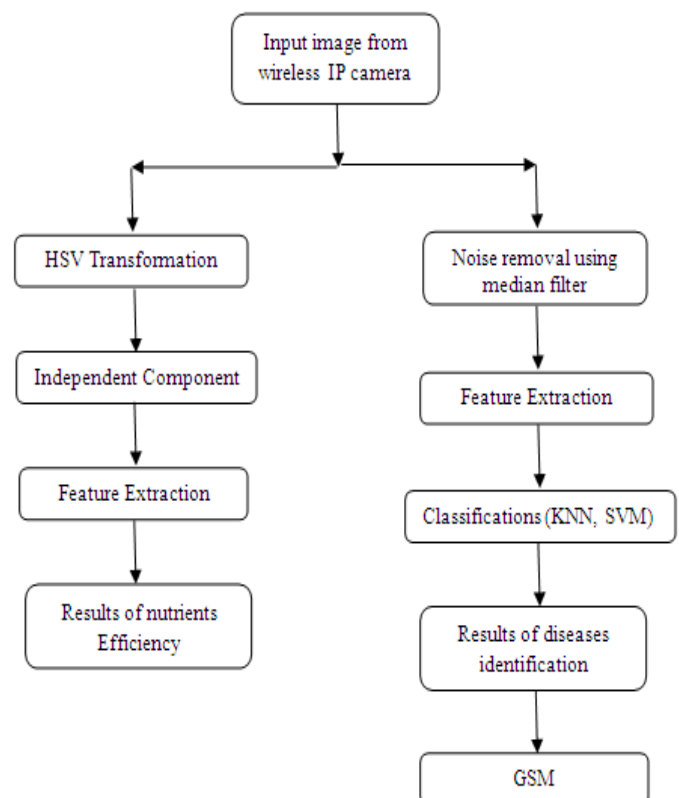


Fig.1. Block diagram of proposed approach

In this paper proposed a novel approach to identify the deficiency of nutrients. The proposed system divides the system into preprocessing, feature extraction and regression. Classification system provides lack of transparency in result and also it is computationally expensive one. To overcome this, implement or introduce the regression method that regression model is tied to each variable and give the predicted value. Better predictions are done using multivariate regression. The main thing to use regression than classification is predict the value of one variable given the value of another and learn how to control future values of a variable by controlling values of variables it's related it.

A. HSV Color Transformation

The HSV color space is essentially completely different from the wide noted RGB color space since it separates out the Intensity (luminance) from the color data (chromaticity). Again, of the two chromaticity axes, a distinction in Hue of a element is found to be visually a lot of distinguished compared to it of the Saturation. For every element, either its Hue or the Intensity is chosen because the dominant feature supported its Saturation.

In situations where color description plays an integral role, the HSV color model is often preferred over the RGB model. The HSV model describes colors similarly to how the human eye tends to perceive color. RGB defines color in terms of a combination of primary colors, whereas, HSV describes color using more familiar comparisons such as color, vibrancy and brightness.

The significance of HSV over RGB is been clearly illustrated in. The approximation done by the RGB feature blurs the distinction between two visually separable colors by changing the brightness. But, the HSV based approximation can determine the intensity and shade variations near the edges of an object, thereby sharpening the boundaries and retaining the color information of each pixel. This makes the HSV-based features very useful in image analysis. So, this approach uses HSV color transformation approach.

Initially, the RGB images of maize crop leaves are acquired. Then, RGB images are converted into Hue Saturation Value (HSV) color space representation. Hue is a color attribute that describes pure color as perceived by an observer. Saturation refers to the relative purity or the amount of white light added to hue and Value means amplitude of light. Considering that (I) exists in RGB color space, then

$$mx_{(i,j)} = \max(I_{R(i,j)}, I_{G(i,j)}, I_{B(i,j)}) \quad (1)$$

$$\min_{(i,j)} = \min(I_{R(i,j)}, I_{G(i,j)}, I_{B(i,j)}) \quad (2)$$

$$H(i,j) = \begin{cases} \frac{60 * (I_{G(i,j)} - I_{B(i,j)})}{mx - \min} & I_{R(i,j)} > \max(I_{G(i,j)}, I_{B(i,j)}) \\ \frac{180 * (I_{B(i,j)} - I_{R(i,j)})}{mx - \min} & I_{G(i,j)} > \max(I_{R(i,j)}, I_{B(i,j)}) \\ \frac{300 * (I_{R(i,j)} - I_{G(i,j)})}{mx - \min} & I_{B(i,j)} > \max(I_{R(i,j)}, I_{G(i,j)}) \end{cases} \quad (3)$$

$$V(i,j) = [mx] \quad (4)$$

$$S(i,j) = \frac{[mx - \min]}{mx} \quad (5)$$

After the transformation process, the Hue component is taken for further analysis. Saturation and Value are dropped since it does not give extra information.

B. Histogram Equalization for Image Enhancement

Histogram Equalization is a technique that generates a gray map which changes the histogram of an image and redistributing all pixels values to be as close as possible to a user –specified desired histogram. HE allows for areas of

lower local contrast to gain a higher contrast. Histogram equalization automatically determines a transformation function seeking to produce an output image with a uniform Histogram. Histogram equalization is a method in image processing of contrast adjustment using the image histogram. This method usually increases the global contrast of many images, especially when the usable data of the image is represented by close contrast values. Through this adjustment, the intensities can be better distributed on the histogram. Histogram equalization accomplishes this by effectively spreading out the most frequent intensity values. Histogram equalization automatically determines a transformation that produces an image with uniform histogram of intensity values. Consider a discrete grayscale image $\{x\}$ and let n_i be the number of occurrences of gray level i . The probability of an occurrence of a pixel of level i in the image is

$$P_x(i) = p(x = i) = \frac{n_i}{n}, 0 \leq i \leq L \quad (6)$$

Where L being the total number of gray levels in the image, n being the total number of pixels in the image, and $P_x(i)$ is the image's histogram for pixel value i , normalized to $[0,1]$. Let us also define the cumulative distribution function corresponding to P_x as

$$cdf_x(i) = \sum \quad (7)$$

$$cdf_x(i) = \sum_{j=0}^i P_x(j) \quad (8)$$

This is also the image's accumulated normalized histogram. A transformation of the form $y = T(x)$ is created to produce a new image $\{y\}$, such that its CDF will be line arid across the value range, i.e.

$$cdf_y(i) = iK \quad (9)$$

For some constant K . The properties of the CDF allow us to perform such a transform; it is defined as

$$y = T(x) = cdf_x(x) \quad (10)$$

The function T maps the levels into the range. The above describes histogram equalization on a grayscale image. However it can also be used on color images by applying the same method separately to the Red, Green and Blue components of the RGB color values of the image. The image is first converted to another color space, HSL/HSV color space in particular, and then the algorithm can be applied to the luminance or value channel without resulting in changes to the hue and saturation of the image. The color intensities are spread uniformly leaving hues and saturation unchanged

C. Independent component analysis

Suppose that we observe a m -dimensional zero mean input signal at time t , $v(t) = \{v_1, \dots, v_m\}'$ where, means the transposition of matrices and vectors. Then the n -dimensional whitening signal, $x(t)$, is given by the following equation:

$$x(t) = Mv(t) = D^{-1/2} E' v(t) \quad (11)$$

The function T maps the levels into the range. The above describes histogram equalization

Where M means a $n \times m$ ($n \leq m$) whitening matrix that is given by a matrix of eigenvalues, D, and a matrix of eigenvectors, E. Here, assume that $v(t)$ is composed of n statistically independent signals,

$$s(t) = \{s_1(t), \dots, s_n(t)\}' \quad (12)$$

Then, the following linear transformation from $x(t)$ to $s(t)$ exists:

$$s(t) = Wx(t) \quad (13)$$

$W = \{w_1, \dots, w_n\}$ is often called a separating matrix, and it can be acquired through the training of a two-layer feed forward neural network. This neural network has n outputs denoted as $\hat{s}(t) = \{\hat{s}_1(t), \dots, \hat{s}_n(t)\}'$ and the i th row vector, w_i' ($i = 1, \dots, n$), of W corresponds to a weight vector from inputs to the i th output \hat{s}_i .

The term 'independent' is used here according to the following definition in statistics:

$$p[s_1(t), \dots, s_n(t)] = \prod_{i=1}^n p[s_i(t)] \quad (14)$$

Where $p[\cdot]$ is a probability density function. Since the above probability density function is not preliminary unknown, suitable objective functions should be devised such that neural outputs, \hat{s}_i are satisfied with Eq. (14) as much as possible, that

$\hat{s}(t) \approx s(t)$. Karhunen and Oja have proposed the following objective function to be maximized in terms of output signals \hat{s} :

$$J(\hat{s}) = \sum_{i=1}^n \left| E\{s_i^4\} - 3[E\{s_i^2\}]^2 \right| \quad (15)$$

Where $E\{\cdot\}$ means expectation. As well known, Eq. (15) corresponds to the fourth-order cumulates of $\hat{s}_i(t)$ called kurtosis. Learning algorithms for a separation matrix, W , are derived from the gradient of Eq. (15). In the followings, we adopt Fast ICA algorithm proposed by Hyvarinen & Oja in which fixed points of the gradient are obtained on-line

D. Feature extraction

The most common visual features include color, texture, shape and etc. Most image annotation and retrieval systems have been constructed based on these features. However, their performance is heavily dependent on the use of image features. In this thesis, texture features are extracted to recognize an avian pox disease.

TABLE.1. Extracted features

GLCM features	Formula	Statistical features	Formula
Contrast	$\sum_{i,j} i-j ^2 p(i,j)$	Mean	$\bar{x} = \frac{1}{n} \sum_{i=1}^n x_i$

Energy	$\sum_{i,j} p(i,j)^2$	Standard Deviation	$s = \sqrt{\frac{1}{n} \sum_{i=1}^n (x_i - \bar{x})^2}$
Entropy	$\sum_{i,j} p(i,j) \log_2 p(i,j)$	Kurtosis	$k = \frac{E(x - \mu)^4}{\sigma^4}$
Homogeneity	$\sum_{i,j} \frac{p(i,j)}{1 + i-j }$	Skewness	$s = \frac{E(x - \mu)^3}{\sigma^3}$
Correlation	$\sum_{i,j} \frac{(i - \mu_i)(j - \mu_j)p(i,j)}{\sigma_i \sigma_j}$		

E. Support Vector Machine (GRBF)

The Support Vector Machine (SVM) is a widely used for classification and regression analysis. It is a supervised learning models associated with learning algorithms that analyze data and recognize the patterns. It was first introduced in the 1992 by Boser, Guyon, and Vapnik (1992). The initial form of SVMs is a binary classifier where the output of learned function is either positive or negative. An input space represented by $X = x_1, x_2, \dots, x_d$ is classified to output space, which is represented by $\{C_1, C_2, \dots, C_j\}$. To classify the data in input space, SVM tries to find the optimal separating hyperplane among all possible separating hyper planes. So, it maximizes the margin and obtains good generalization ability. A separating hyperplane is a linear function that can separate the training data into two classes (Class1=+1 and Class2=-1) in the separable feature space, as shown in Figure 3

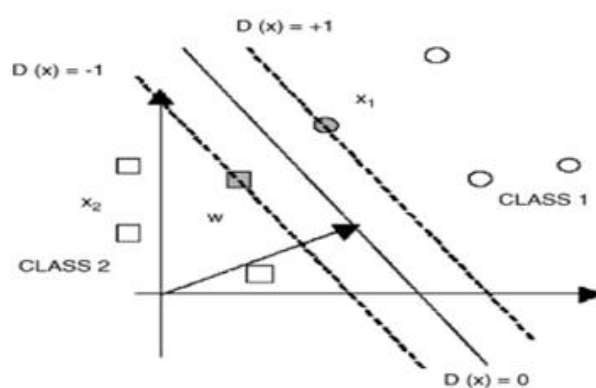


Fig.3. SVM Classification

The following function describes a separating hyperplane function

$$D(x) = (\omega * x) + \omega_0 \quad (16)$$

All separating hyperplanes must satisfy the following equation:

$$Y_i[(\omega * x_i) + \omega_0] \geq 1 \quad i = 1, \dots, n \quad (17)$$

In this paper we used the kernel function while developing

SVM model. Gaussian kernels are used to modify the input space into high dimensional feature space. The kernels having the following equation.

$$K(x_i, x_j) = e^{-\|x_i - x_j\|^2 / 2\sigma^2} \quad (18)$$

In this paper, Gaussian radial basis function kernel function is used.

F. K-Nearest Neighbors classification method (KNN)

The KNN classification algorithm is a supervised method with a desirable computational speed along with the acceptable classification accuracy. The KNN-based classifier does not require the train stage and is based on a simple theory and mathematics. The structure of the KNN classifier imposes lower computational burden.

In order to formulate the KNN classification algorithm, suppose that the pair $(x_i, \delta(x_i))$ contains the feature vector x_i and its corresponding label $\delta(x_i)$ where $\delta \in \{1, 2, \dots, n\}$ and $i = 1, 2, \dots, N$ (n and N are the number of classes and the number of train feature vectors, respectively). For an arbitrary feature vector x_j , calculation of a defined distance between this feature and the feature vector $x_{i,j}$ is possible as follows,

$$d(i, j) = f(X_i, X_j) \quad (19)$$

Where $f(X_i, X_j)$ is a scalar distance function. For instance, $f(X_i, X_j)$ can be defined as

$$\begin{cases} (a) f(X_i, X_j) = (X_i - X_j)^T \sum (X_i - X_j) \\ (b) f(X_i, X_j) = \left(\sum_{k=1}^p (X_i(k) - X_j(k))^r \right)^{1/r} \\ (c) f(X_i, X_j) = \frac{1}{p} \sum_{k=1}^p \text{abs}(X_i(k) - X_j(k)) \end{cases} \quad (20)$$

Where the first term of the Eq. (5) called generalized distance and for the weight matrix $\sum = 1$ the famous Euclidean norm will be achieved. While the second term of the Eq. (5) is called Minkovski distance of degree r and for $r = 2$, again the Euclidean distance appears. The third term of Eq. (5) is called the City Block distance and is used in many pattern recognition cases. If the distance vector $D(i)$ is defined by following equation

$$D(i) = \{d(i, j) | i = 1, 2, \dots, N_{\text{train}}\} \quad (21)$$

By sorting the $D(i)$ vector in an ascending fashion, and choosing the first K elements (which is called K nearest neighbors) as follows

$$D_N(i) = \text{sort}(D(i)) \quad (22)$$

$$V = \{\delta(D_N(i)(1)), \dots, \delta(D_N(i)(K))\} \quad (23)$$

According to the KNN algorithm, the test feature x_i belongs to the class with the major votes in the K -nearest vote vector V . In order to determine the optimum K corresponding to the best accuracy, a simple way is to alter the K from 1 to a large enough value (in this paper $k=10$) and choosing the K for which the best accuracy is obtained for all test features.

Results and Discussion

The acquired image is having some kind of noise due to transmission. This noise is removed using median filter. The texture features are extracted for the preprocessed image using GLCM and mean, standard deviation, kurtosis and skewness. The feature extraction results are shown in table 2 to table 6.

TABLE .II. GLCM features for normal paddy

S. No	Entropy	Contrast	Correlation	Energy	Homogeneity
IMAGE 1	6.8403	0.0673	0.9875	0.5702	0.9732
IMAGE 2	6.3220	0.0783	0.9862	0.4031	0.9762
IMAGE 3	6.8293	0.582	0.9858	0.4830	0.9763
IMAGE 4	6.2015	0.0341	0.9881	0.5165	0.9832

TABLE .III. Mean, standard deviation, kurtosis and skewness features for normal paddy

S. No	Mean	Standard Deviation	Kurtosis	Skewness
IMAGE 1	149.3516	3.0039	684.2631	-11.0540
IMAGE 2	148.5908	3.7355	690.5899	-12.7127
IMAGE 3	148.7042	3.5482	687.6249	-12.0819
IMAGE 4	148.9201	3.8028	694.8445	-12.5141

TABLE .IV. GLCM features for Zinc deficiency

S.No	Entropy	Contrast	Correlation	Energy	Homogeneity
IMAGE 1	7.8149	0.6178	0.9085	0.0731	0.8224
IMAGE 2	7.8146	0.6171	0.9078	0.0726	0.8219
IMAGE 3	7.8039	0.6133	0.9054	0.0619	0.8102
IMAGE 4	7.8152	0.6182	0.9088	0.0736	0.8235

TABLE IV. Mean, standard deviation, kurtosis and skewness features for Zinc deficiency

S.No	Mean	Standard Deviation	Kurtosis	Skewness
IMAGE 1	160.3277	2.8723	72.3196	-2.6600
IMAGE 2	160.3270	2.8853	71.3006	-2.7650
IMAGE 3	160.3370	2.8053	74.3126	-2.5550
IMAGE 4	160.3290	2.8967	72.9854	-2.6168

TABLE .V. GLCM features for mycorellosiellaoryzae

S.No	Entropy	Contrast	Correlation	Energy	Homogeneity
IMAGE 1	7.8037	0.6130	0.9052	0.0619	0.8101
IMAGE 2	7.8147	0.6174	0.9080	0.0729	0.8228
IMAGE 3	7.8141	0.6165	0.9072	0.0721	0.8214
IMAGE 4	7.8138	0.6161	0.9069	0.7118	0.8210

TABLE VI. Mean, standard deviation, kurtosis and skewness features for mycorellosiellaoryzae

S.No	Mean	Standard Deviation	Kurtosis	Skewness
IMAGE 1	160.3316	2.8677	75.6889	-2.5019
IMAGE 2	160.3308	2.8904	75.6991	-2.5010
IMAGE 3	160.3435	2.7841	76.3897	-2.4978
IMAGE 4	160.3455	2.7741	76.4298	-2.3697

The above feature extraction results are given as an input to the classifiers. In this paper KNN and SVM (GRBF) classifiers are used. The performance metrics are used for evaluating the classifiers. Cross Validation and confusion matrices are used to evaluate the performance of the classifiers. In this paper a 10 fold cross validation is used.

TABLE. VII. A confusion matrix

Actual Value	Predicted Value	
	Negative	Positive
Negative	TN	FN
Positive	FP	TP

$$\text{Accuracy} = \frac{TP + TN}{TP + TN + FP + FN}$$

$$\text{Specificity} = \frac{TN}{TN + FP}$$

$$\text{Sensitivity} = \frac{TP}{TP + FN}$$

$$\text{PositivePredictiveValue (PPV)} = \frac{TP}{TP + FP}$$

$$\text{NegativePredictiveValue (NPV)} = \frac{TN}{TN + FN}$$

TN (True Negative) – Correct Prediction as normal

FN (False Negative) – Incorrect prediction of normal

FP (False Positive) – Incorrect prediction of abnormal

TP (True Positive) – Correct prediction of abnormal

The overall effectiveness of the system can be measured by using accuracy. The accuracy which computes the proportion between correctly classified samples and total samples. Sensitivity and specificity are the most widely used statistics to describe a diagnosis test. Sensitivity measures the proportion of actual positives which are correctly identified as positives. Specificity measures the proportion of actual negatives which are correctly identified. (i.e) The sensitivity and specificity are used to approximate the probability of the positive and negative label being true. Positive predictive value indicates the positive results which were correctly predicted.

The graph is plotted for accuracy, specificity, sensitivity, PPV and NPV of zinc deficiency paddy image is shown in figure 4.

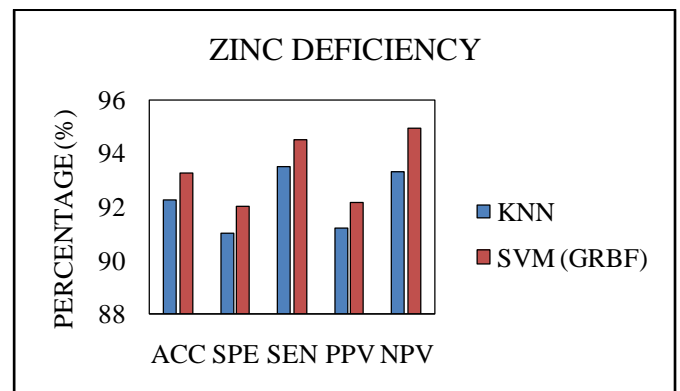


Fig.4. Performance metrics for zinc deficiency paddy image

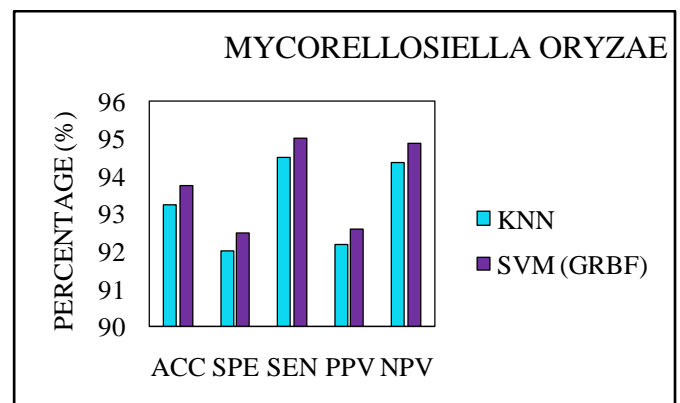


Fig.5. Performance metrics for Mycorellosiellaoryzae paddy image

The experimental process is conducted in LabVIEW. Total 60 images are collected from open source, in those 30 images for training purpose and 30 images for testing purpose. These total images are collected from the open source.



Fig.6.Deficiency Part

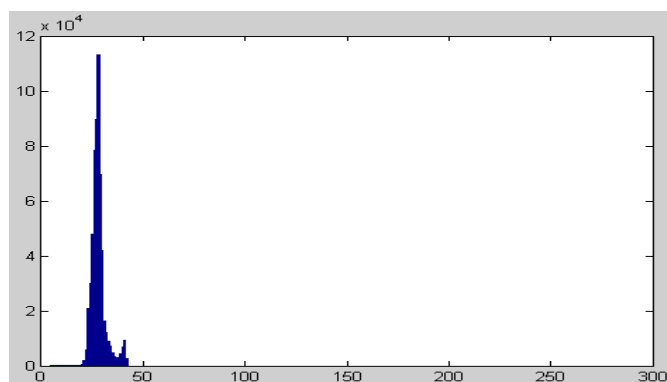


Fig.7. Histogram Plot

Result values for training dataset –Phosphorous

	1	2	3	4	5	6	7
1	0	0	0	0	0	0	0
2	0	0	0	0	0	0	0
3	0	0	0	0	0	0	0
4	0	0	0	0	0	0	0
5	0	0	0	0	0	0	0
6	3.1780e-15	-1.6051e-04	-0.0636	-0.1143	0.0134	-0.0550	-0.0370
7	5.4123e-15	-2.7180e-04	-0.1077	-0.1935	0.0227	-0.0931	-0.0626
8	7.7161e-15	-3.3093e-04	-0.0518	-0.0781	-0.0088	0.1129	-0.0384
9	1.1713e-14	-5.1296e-04	-0.0963	-0.1528	-0.0062	0.1294	-0.0671
10	6.9944e-15	-8.2451e-04	0.0524	0.4687	-0.1054	0.2754	-0.0439
11	-6.8834e-15	0.0018	0.1546	0.7747	-0.0789	0.2257	0.0491
12	1.1324e-14	0.0026	-0.1641	-0.6806	0.1119	0.1296	-0.0051
13	9.9920e-15	0.0021	0.0788	-0.1642	-0.0049	0.6023	0.0924
14	-6.8834e-15	-9.9772e-04	-0.0257	0.5035	-0.0879	-0.4955	-0.1319
15	7.7716e-15	-0.0089	-0.2084	0.0070	-0.0849	0.4622	-0.1540
16	-2.5313e-14	0.0091	-0.0268	-0.1042	0.2296	-0.3749	0.1613
17	4.9738e-14	-0.0098	0.1223	0.4438	-0.3891	1.6297	-0.1510
18	-8.6597e-15	0.0138	0.1115	-0.3674	0.2263	0.0138	0.2577
19	-8.8818e-15	0.0164	0.1123	0.1485	0.1324	-1.2043	0.0261
20	1.5543e-14	-0.0105	-0.1353	0.2841	-0.1574	0.6890	-0.1931

Testing Values of Phosphorus

	1	2	3	4	5
1	0				
2	0				
3	0				
4	0				
5	0				
6	0				
7	0				
8	0				
9	0				
10	0				
11	0				
12	3.7360				
13	4.8218				
14	4.8563				
15	5.7617				
16	5.9559				
17	10.3748				
18	10.2803				
19	13.7916				
20	11.4437				
21	6.3946				
22	5.4872				
23	3.1746				
24	2.1224				
25	0				
26	0				
27	0				

Testing value of Nitrogen

	1	2	3	4	5	6
16	0					
17	0					
18	0					
19	0					
20	0					
21	0					
22	0					
23	0					
24	0					
25	0					
26	0					
27	0					
28	0					
29	3.9354					
30	18.2513					
31	32.7218					
32	22.5709					
33	12.0456					
34	3.7971					
35	0					
36	0					
37	0					
38	0					
39	0					
40	0					
41	0					
42	0					
43	0					

TABLE. VII. Comparison of Accuracy

Techniques	Correctly detected Images	Accuracy
PCA	26/30	86
ICA	27/30	90
MPLS	28/30	93.3

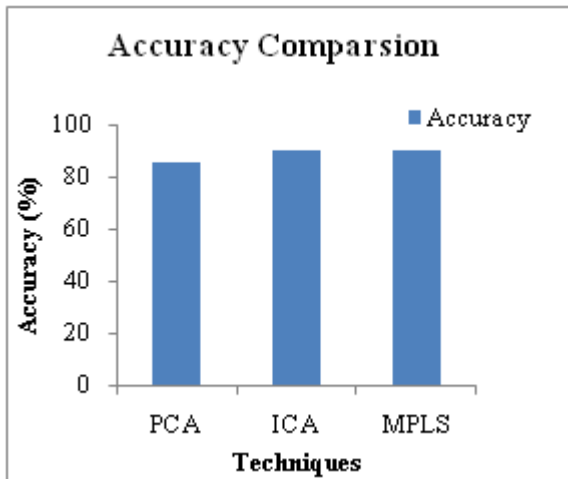


Fig.6.Comparison of Accuracy

Conclusion

In this paper, paddy and wheat diseases are identified with the help of SVM (GRBF) and KNN classifiers. Texture features such as GLCM and mean, standard deviation, kurtosis and skewness features are extracted. This paper use a MPLS approach for detects the nutrient deficiency in leaf image. Three steps are carried over in this paper they are preprocessing, feature extraction and regression. ICA technique is more natural than PCA method. Compared to PCA and ICA, proposed MPLS is evaluating more for dimensionality reduction. From the experimental result it is clearly observed that the proposed method provides better result than existing method.

References

- [1] Georges Giraud, "The World Market of Fragrant Rice, Main Issues and Perspectives", International Food and Agribusiness Management Review, Vol. 16(2), 2013.
- [2] Arendonk, J.J.C.M., Niemann, G.J., Boon, J.J., Lambers, H., 1997.Effects of nitrogen supply on the anatomy and chemical composition of leaves of four grass species belonging to the genus Poa, as determined by image-processing analysis and pyrolysis-mass spectrometry. Plant Cell Environ. 20, 881-897.
- [3] J. A. Silva and R. Uchida, "Essential Nutrients for Plant Growth: Nutrient Functions and Deficiency Symptoms", College of Tropical Agriculture and Human Resources, University of Hawaii at Manoa, 2000.
- [4] Hirose, T., Freijsen, AHJ and Lambers, H. "Modelling of response to nitrogen availability of two plantago species growth at a range of exponential nutrient addition rates. Plant, Cell and Environment 11, 827-834.
- [5] Lambers, H and Poorter, H. "Inherent variation in growth rate between higher plants: A search for physiological causes and ecological consequences. Advances in Ecological Research 23, 187-261.
- [6] Corn leaf analysis and interpretative Guidelines, Olsen's Agricultural Laboratory, Inc, 2008.
- [7] SantanuPhadikar, Jaya Sil and Asit Kumar Das, "Rice diseases classification using feature selection and rule generation techniques", Computer and Electronics in Agriculture, Vol. 90, pp. 76-85, 2013.
- [8] Gonzalez R.C and Woods R.E, Digital Image Processing, Prentice Hall, New Jersey, 2002.
- [9] R. Haralick, K. Shanmugam and I. Dinstein, "Texture Features For image Classification", IEEE Transaction, SMC, Vol.3, issue 3, page no:610-621,1973.
- [10] Du, D. Huang, X. Wang, and X. Gu, "Computer-aided plant species identification (CAPSI) based on leaf shape matching technique," Transactions of the Institute of Measurement and Control. 28, 3 (2006) pp. 275-284.
- [11] Lemaire, G. Diagnostic Tool (s) for Plant and Crop N Status. Theory and Practice for Crop N Management. In Proceedings of the 15th N Workshop "Towards a Better Efficiency in N use", Lleida, Spain, 28-30 May 2007; pp. 15-29.
- [12] Netto, A.T., Campostrin, E., Gonc, J., , Oliveira, A., Bressan-Smith,R.E., 2005. Photosynthetic pigments, nitrogen, chlorophyll afluorescence and SPAD-502 readings in coffee leaves. Sci.Hortic. 104, 199-209.
- [13] Carter, G.A., Knapp, A.K., 2001. Leaf optical properties in higher plants linking spectral characteristics to stress and chlorophyll concentration. Am. J. Bot. 88 (4), 677-684.
- [14] Edmeades, D. C. 2003. The long-term effects of manures and fertilizers on soil productivity and quality: a review. Nutr.Cycl. Agroecosyst. 66: 165-180.
- [15] Saleque, M. A., Abedin, M. J., Bhuiyan, N. I., Zaman, S. K.and Panaullah., G. M. 2004. Long-term effects of inorganic and organic fertilizer sources on yield and nutrient accumulation of lowland rice. Field Crop Res. 86: 53-65.